Novel Schemes for Repeatable Runout Compensation Using Adaptive Feedforward Cancellation

Shang-Chen Wu and Masayoshi Tomizuka
Department of Mechanical Engineering
University of California
Berkeley, CA 94720
scwu@berkeley.edu, tomizuka@me.berkeley.edu

ABSTRACT

In this report, new methods to estimate repeatable runout (RRO) in hard disk drives are described. The techniques are based on adaptive feedforward cancellation (AFC). To enhance the performance, the modified Filtered-X LMS (MFX-LMS) adaptive algorithm is combined with a Kalman filter. The estimation of RRO in this report is to be performed at the manufacturing stage. The estimated data are used in real-time control to generate the compensation signal which cancels RRO disturbances. The proposed method is compared with other common methods for handling RRO by simulations. In addition, an frequency selective estimation is proposed to exclude the high frequency components of RRO in the estimation process. Simulation results show the effectiveness of the proposed schemes and the resulting reduction of position errors in the track following mode.

I. INTRODUCTION

With the continuously increasing storage capacity of hard disk drives (HDDs), the track density on the disk becomes higher and higher. This makes it a challenge to accurately position the disk drive's read/write head (R/W head) in the presence of several disturbances. In the sector servo

system for HDDs, a circular disk is divided into equally sized angular pieces (called sectors) whose boundaries are servo fields. A set of servo fields defines a servo-written track center. The position error signal (PES) indicating the deviation of the R/W head from the servo-written track center is obtained from each servo field as the R/W head passes through.

The top view of a disk is shown in Fig. 1. In track following operations, the R/W head normally follows a data track with reference to a servo-written track center. The servo-written track center is typically not a perfect centric circle, since the servo fields may be placed on either side of the ideal track center due to disturbances in the servo-writing process. The difference between a servo-written track center and an ideal circular track center introduces written-in errors, which are often referred to as repeatable runout (RRO) errors or written-in repeatable runout (WI-RRO) errors since they cause the same errors each time the head follows the track. RRO is periodic and synchronized with disk rotation. The other type of disturbances called non-repeatable runout (NRRO) is caused by disk vibrations, windage, noise and so on.

A great deal of research effort has been focused on the RRO compensation. In [1]–[4], the controllers make the R/W head follow the servo-written track center. This might cause problems

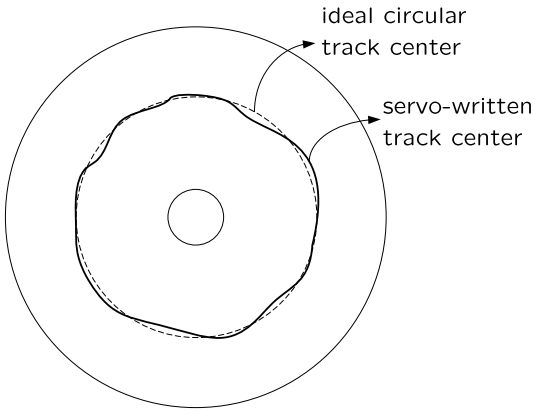

Fig. 1. Servo-written track center v.s. ideal circular track center

when the RRO disturbance is not coherent at different tracks. In particular, with two adjacent tracks, when written-in error of the inner track and that of the outer track point outwards and inwards, respectively, the two track paths could interfere with each other, which may result in data corruption. To prevent this from happening, another type of control scheme has been considered [5], [6]. During manufacture of a disk drive, after servo-writing process, a table which includes a series of compensation values for RRO with respect to the positions of servo fields is calculated and stored. Then, during normal operations of the disk drive by the user, the compensation table is utilized to construct an additional input into the servo control loop to correct the servo-written track centers so that they are closer the ideal circular track centers. Improvement achieved by this scheme depends on the accuracy of RRO estimation. Estimating the RRO disturbance for every track of the disk requires a significant amount of manufacturing time. Therefore, the motivation for this research is to develop a technique which can achieve rapid and accurate estimation of RRO disturbance in disk drives.

Adaptive feedforward cancellation (AFC) has been widely applied in HDD industry to reduce periodic disturbances [2]–[4]. In these methods, the periodic disturbance is modeled as a sum of several sinusoids of known frequencies and the unknown amplitudes and phases are estimated by an adaptive algorithm. The method is effective when dealing with a few selected harmonics. However, it is impractical to compensate for a large number of harmonics due to the constraint of computation power. In [7] and [8], the authors proposed advanced methods to estimate all harmonics in RRO disturbance. The methods are based on AFC but do not require intensive computations. In this report, modifications of the previous schemes are proposed to enhance the estimation performance. The remainder of this report is organized as follows. In Section II, the design schemes from the previous report [8] are briefly reviewed. Then a modified scheme

is proposed to improve the estimation performance. Section III describes an HDD application of the modified scheme for RRO estimation. The AFC and modified methods are compared with other common methods for handling RRO: the inverse sensitivity method and the repetitive control method. In Section IV, a frequency selective estimation scheme is proposed to exclude the high frequency components of RRO in the estimation process. Finally, conclusions are given in Section V.

II. General Problem Formulation and AFC Configuration

A block diagram of a general single-input-single-output (SISO) linear time invariant (LTI) discrete-time feedback control system with periodic disturbances is shown in Fig. 2. In the figure, $P(z)$ denotes the plant and $C(z)$ the feedback controller. The reference $r(k)$ and the disturbance $d(k)$ are periodic with period N. Without loss of generality, $r(k)$ is assumed to be zero. The periodic disturbance $d(k)$ is compensated by injecting an additional compensation signal $\widehat{d}(k)$, which is an estimation of $d(k)$, at the reference to minimize its effect on the error signal $e(k)$. Performance of the disturbance cancellation depends on the accuracy of its estimation. The disturbance can be estimated or learned from the error signal $e(k)$ on which the

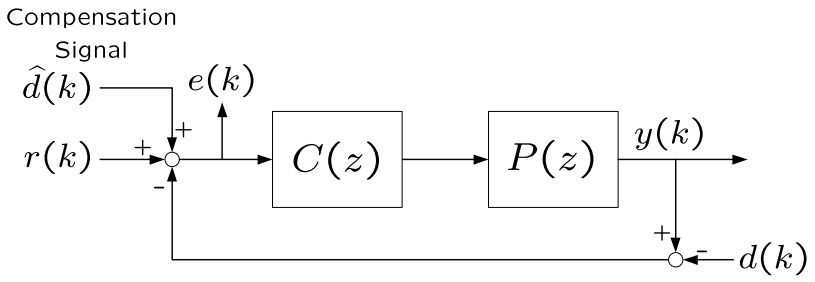

Fig. 2. Block diagram of feedback control system with periodic measurement disturbance $d(k)$

effects of $d(k)$ and $\widehat{d}(k)$ are given by

$$e(k) = S(z)\left[d(k) - \widehat{d}(k)\right], \quad S(z) = \frac{1}{1 + P(z)C(z)}. \tag{1}$$

where $S(z)$ is the sensitivity function of the closed-loop system.

A. Standard AFC

A block diagram description for an AFC scheme to estimate the periodic disturbance $d(k)$ is presented in Fig. 3. The AFC scheme shown inside the dashed lines is an add-on structure to the feedback system in Fig. 2. Therefore, it does not require to alter the original feedback configuration.

The AFC scheme consists of two major elements: a digital filter, $W(z)$, and an adaptive algorithm, LMS (Least-Mean-Square) block. It aims to generate an $\widehat{d}(k)$ to follow the periodic disturbance $d(k)$. The adaptive algorithm adjusts the coefficients of the filter to minimize the mean-square value of the error signal $e(k)$. The input signal $x(k)$ is an excitation to the adaptive

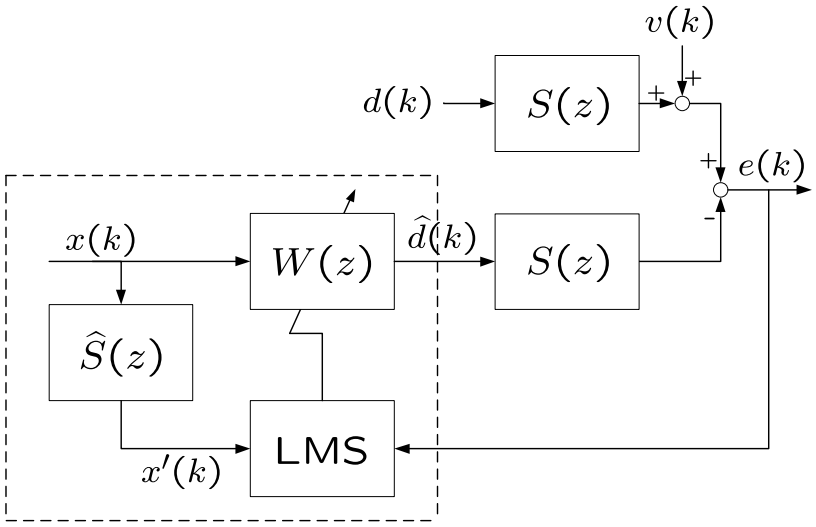

Fig. 3. Block diagram of FXLMS

filter and is chosen to be highly correlated to $d(k)$. $v(k)$ represents uncorrelated noise components which appear in $e(k)$. Notice that $e(k)$ is not the true error between $d(k)$ and $\widehat{d}(k)$, but only the filtered version of it, as shown in Eq. (1). For this kind of system, $x(k)$ must also be filtered by $S(z)$, before it is utilized by the LMS algorithm, to ensure convergence. Because of the filtering notion, the adaptive algorithm is called the Filtered-X LMS (FX-LMS) algorithm. In practical applications, $S(z)$ is unknown and an approximation $\widehat{S}(z)$ is utilized, with impulse response $\widehat{s}(k)$. A popular choice for the adaptive filter is a finite impulse response (FIR) digital filter, since FIR filters are always stable.

Let the FIR filter $W(z)$ has length N, which is the period of $d(k)$, i.e.

$$W(z) = w_0 + w_1 z^{-1} + \cdots + w_{N-1} z^{-N+1}.$$

Then, the adaptive feedforward compensation with FX-LMS algorithm can be described by the following equations:

$$z(k) = \mathbf{x}^T(k)\mathbf{w}(k), \tag{2}$$

$$\mathbf{x}'(k) = \widehat{s}(k) * \mathbf{x}(k), \tag{3}$$

$$\mathbf{w}(k+1) = \mathbf{w}(k) + \mu \mathbf{x}'(k) e(k), \tag{4}$$

where

$$\mathbf{x}(k) = \begin{bmatrix} x(k) & x(k-1) & \cdots & x(k-N+1) \end{bmatrix}^T \tag{5}$$

$$\mathbf{x}'(k) = \begin{bmatrix} x'(k) & x'(k-1) & \cdots & x'(k-N+1) \end{bmatrix}^T \tag{6}$$

$$\mathbf{w}(k) = \begin{bmatrix} w_0(k) & w_1(k) & \cdots & w_{N-1}(k) \end{bmatrix}^T \tag{7}$$

From Fig. 3, $z(k) = \widehat{d}(k)$ is the output of the adaptive filter, $\mathbf{x}(k)$ is the input signal vector, $\mathbf{x}'(k)$ is the filtered input signal vector, $\mathbf{w}(k)$ is the filter coefficients at time k in vector form, μ is the step size, and $*$ denotes the convolution sum. Define the fundamental and harmonic frequencies $f_k \in \Omega$ where

$$\Omega = \left\{ f_k \mid f_k = \frac{k}{T_s N}, k = 1, \cdots, \left\lfloor \frac{N}{2} \right\rfloor \right\} \tag{8}$$

In frequency domain, $d(k)$ contains frequency components only at frequencies $f_k \in \Omega$. Therefore, the input signal $x(k)$ is chosen as an impulse train with period N, i.e.

$$x(k) = \begin{cases} 1, & \text{if mod}(k, N) = 0 \\ 0, & \text{otherwise.} \end{cases} \tag{9}$$

Notice that $x(k)$ contains the required frequency components for the adaptive filter $W(z)$ to generate the corresponding estimate components of $d(k)$. Because of the sparse natural of the signal $x(k)$, the computation of the FX-LMS algorithm is simplified. $x(k)$ is like a circular pointer which points to each coefficient of $W(z)$ sequentially to be the output $z(k)$. Hence, no computation is required in Eq. (2). Equation (3) can be pre-calculated, since $\widehat{s}(k)$ and $\mathbf{x}(k)$ are known beforehand. Assume $\widehat{s}(k)$ has length L. Then, $\mathbf{x}'(k)$ contains L non-zero elements. Therefore, from Eq. (4), only L coefficients in $W(z)$ need to be updated at every sampling time. With a small length of $\widehat{s}(k)$, the computational load is practical for implementation.

Ideally, when there is no uncorrelated noise, $v(k) = 0$, perfect estimation can be achieved by producing $z(k) = d(k)$ such that $e(k) = 0$. The filter coefficient vector $\mathbf{w}(k)$ will converge to an optimal solution $\mathbf{w}^o$. However, in most practical applications, $v(k) \neq 0$. By defining a

coefficient error vector as

$$\mathbf{e_d}(k) \triangleq \mathbf{w}(k) - \mathbf{w}^o, \tag{10}$$

and using Eq. (4), it is shown that

$$\begin{aligned}
\mathbf{e_d}(k+1) &= \mathbf{e_d}(k) + \mu \mathbf{x}'(k) e(k), \\
&= \mathbf{e_d}(k) + \mu \mathbf{x}'(k)[s(k) * [d(k) - z(k)] + v(k)], \\
&= \mathbf{e_d}(k) + \mu \mathbf{x}'(k)[s(k) * [d(k) - z(k)]] \\
&\quad + \mu \mathbf{x}'(k) v(k)
\end{aligned} \tag{11}$$

The last term $\mu \mathbf{x}'(k) v(k)$ introduces a perturbation to the error equation. This undesirable interference would cause serious degradation in both estimation speed and accuracy when the noise level of $v(k)$ is high. The effect of $v(k)$ is reflected in the adaptive filter output $z(k)$. In other words, the estimation results from the FX-LMS algorithm are buried in the noise. Therefore, it makes sense to apply Kalman filtering to estimate $d(k)$ from the noise contaminated signal $z(k)$.

B. AFC combined with Kalman filter

The structure of AFC with Kalman filtering is in Fig. 4. The periodic disturbance $d(k)$ can be considered as the states of a stochastic process

$$\begin{aligned}
\mathbf{d}(l) &= \mathbf{d}(l-1) \\
\mathbf{z}(l) &= \mathbf{d}(l) + \mathbf{u}(l),
\end{aligned} \tag{12}$$

where

$$\mathbf{d}(l) = [d_0(lN)\ d_1(lN)\ \cdots\ d_{N-1}(lN)]^T$$

$$\mathbf{z}(l) = [z(lN)\ z(lN+1)\ \cdots\ z((l+1)N-1)]^T$$

$$\mathbf{u}(l) = [u(lN)\ u(lN+1)\ \cdots\ u((l+1)N-1)]^T.$$

The time index l represents the number of revolutions. Notice that the adaptive filter output $\widehat{d}(k)$ in Fig. 3 is now interpreted as the actual disturbance $d(k)$ plus the excess noise $u(k)$. By applying standard Kalman filter formula,

$$\begin{aligned} K(l) &= P(l-1)\,[P(l-1)+R]^{-1} \\ \widehat{\mathbf{d}}(l) &= [1-K(l)]\,\widehat{\mathbf{d}}(l-1) + K(l)\,\mathbf{y}(l) \\ P(l) &= [1-K(l)]\,P(l-1). \end{aligned} \tag{13}$$

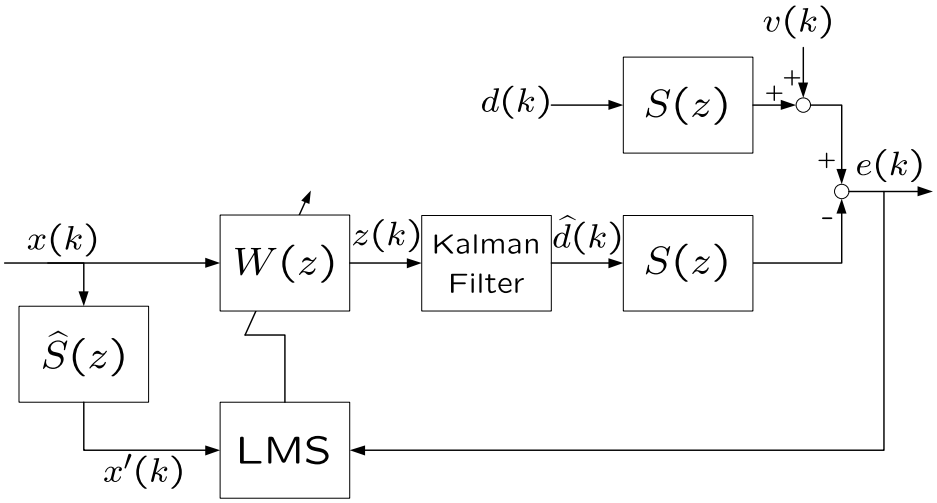

Fig. 4. Block diagram of AFC system with FX-LMS algorithm and Kalman filter

Time-varying Kalman filter gain is utilized to speed up convergence. Since $u(k)$ is introduced by $v(k)$, the noise covariance R can be selected according to the statistical property of $v(k)$ to achieve better estimation results. Assume $R = rI$, then $K(l)$ and $P(l)$ are simplified to scalars, which can be calculated beforehand. Notice that the Kalman filter is operated at a sampling rate N times slower than the system sampling rate. $\widehat{d}(k)$ is obtained from the output of the Kalman filter.

In the LMS algorithm, a larger step size μ results in faster convergence. However, there is an upper bound on μ to maintain stability of the algorithm. It is known that the FX-LMS algorithm suffers from a reduction in maximum step size due to the delay caused by the dynamics system $S(z)$ [9]. The effect of $S(z)$ leads to slower convergence and therefore overall limited performance. As an simplified example, assume $S(z)$ is modeled as a pure delay Δ without modeling error, i.e.

$$S(z) = \widehat{S}(z) = z^{-\Delta}, \tag{14}$$

and no Kalman filter is added in the AFC scheme. Using Eq. (2), the error signal is written as

$$e(k) = d(k-\Delta) - z(k-\Delta) \tag{15}$$

$$= d(k-\Delta) - \mathbf{x}^T(k-\Delta)\mathbf{w}(k-\Delta). \tag{16}$$

Notice that the error signal is computed using the past coefficient vector $\mathbf{w}(k-\Delta)$. Then, Eq.

(4) becomes

$$\mathbf{w}(k+1) = \mathbf{w}(k) + \mu \mathbf{x}(k-\Delta)e(k) \tag{17}$$

$$= \mathbf{w}(k) + \mu \mathbf{x}(k-\Delta)\left[d(k-\Delta) - \mathbf{x}^T(k-\Delta)\mathbf{w}(k-\Delta)\right]. \tag{18}$$

The delayed coefficient vector $\mathbf{w}(k-\Delta)$ in the coefficient update equation results in slow convergence rate. To remove the delay in the coefficient updates, a new error signal is defined

$$\varepsilon(k) \triangleq e(k) + \widehat{s}(k) * z(k) - \mathbf{x}'^T(k)\mathbf{w}(k) \tag{19}$$

$$\tag{20}$$

From Eq. (15), $\varepsilon(k)$ is expressed as

$$\varepsilon(k) = e(k) + z(k-\Delta) - \mathbf{x}^T(k-\Delta)\mathbf{w}(k) \tag{21}$$

$$= d(k-\Delta) - \mathbf{x}^T(k-\Delta)\mathbf{w}(k). \tag{22}$$

The new error signal is computed using $\mathbf{w}(k)$ without delay. The FX-LMS algorithm utilize the error signal $\varepsilon(k)$ is called the Modified Filtered-X LMS (MFX-LMS) algorithm [10]. The MFX-LMS algorithm is able to eliminate the effect of $S(z)$ in the case of no modeling errors, such that the behavior of the system is similar to that of a standard LMS adaptive filter. In this report, an AFC scheme combining MFX-LMS algorithm and Kalman filtering is proposed. Since the MFX-LMS algorithm does not suffer from maximum step size reduction, a larger step size can be selected to increase the convergence speed.

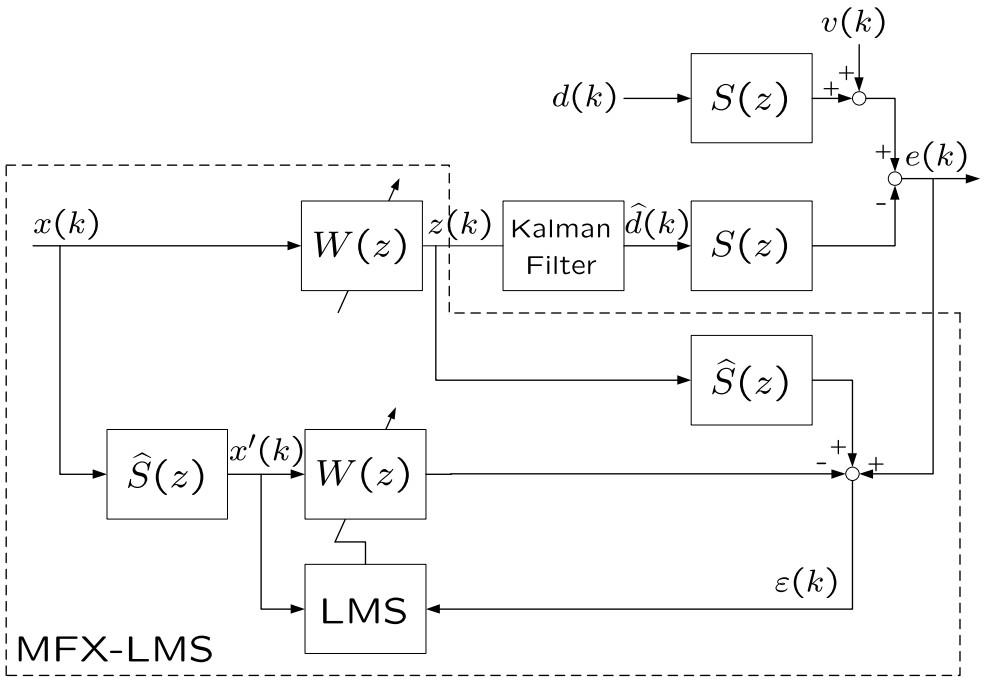

Fig. 5. Block diagram of AFC system with MFX-LMS algorithm and Kalman filter

C. AFC utilize Modified Filtered-X LMS algorithm

The proposed AFC scheme is presented in Fig. 5. It consists of the MFX-LMS algorithm as shown inside the dashed lines and a Kalman filter. The MFX-LMS algorithm can be described by the following equations:

$$z(k) = \mathbf{x}^T(k)\mathbf{w}(k), \tag{23}$$

$$z'(k) = \widehat{s}(k) * z(k), \tag{24}$$

$$\mathbf{x}'(k) = \widehat{s}(k) * \mathbf{x}(k), \tag{25}$$

$$\varepsilon(k) = e(k) + z'(k) - \mathbf{x}'^T(k)\mathbf{w}(k) \tag{26}$$

$$\mathbf{w}(k+1) = \mathbf{w}(k) + \mu\mathbf{x}'(k)\varepsilon(k). \tag{27}$$

The MFX-LMS algorithm removes the effect of the dynamic system $S(z)$ with the expense of additional computations in Eqs. (24) and (26). Since an approximate model $\widehat{S}(z)$ is used, the algorithm have to be robust to model uncertainties. It is shown [11] that the MFX-LMS algorithm is stable as long as it satisfies

$$\mathfrak{Re}\left[\widehat{S}(e^{j\omega T_s})/S(e^{j\omega T_s})\right] > \frac{1}{2}\ , \qquad \text{for } 0 \leq \omega \leq \frac{\pi}{T_s}. \tag{28}$$

In other words, for the case of no phase errors the estimated amplitude should be greater than half of the real one, and for the case of no amplitude errors the phase errors should be less than 60°.

III. Application to RRO Compensation in HDDs

In the track following mode of HDDs, the closed-loop control operates by the feedback of the position error signal (PES) with perturbations from RRO and NRRO disturbances. The objective is to estimate the periodic disturbance RRO, and construct an compensation signal to correct the servo-written track center such that it is closer to an ideal circular track center.

A. Performance comparisons

The track following servo system of HDDs can be represented by the block diagram described in Fig. 2, where the error signal $e(k)$ is the PES measurement and the periodic disturbance $d(k)$ is the RRO. PES can be decomposed in to Repeatable PES (RPES) and Non-Repeatable PES (NRPES) caused by RRO and NRRO respectively. The disk spindle speed in this numerical simulation study is 7200 rpm, which means that the fundamental frequency of RRO is 120 Hz. Pre-recorded RRO and NRRO disturbances for 20 different tracks are used. The level of NRRO has significant impact on the performance. In these data tracks, the ratio between RPES and

NRPES is in the following region,

$$0.64 \leq \frac{\sigma(RPES)}{\sigma(NRPES)} \leq 0.90 \tag{29}$$

with mean value 0.77, where $\sigma(\cdot)$ is the standard deviation. The small ratio and wide range make it challenging to obtain an accurate estimate of RRO with consistent performance.

Existing techniques and the proposed method are applied to estimate RRO. Their performances are evaluated by reduction of RPES after compensation. The effect of RRO on RPES through the sensitivity function is

$$RPES(k) = S(z)d(k), \tag{30}$$

$$RPES_{cmp}(k) = S(z)\left[d(k) - \widehat{d}(k)\right]. \tag{31}$$

The performance index is defined as

$$\Delta\ \sigma(RPES) = \frac{\sigma(RPES_{cmp}) - \sigma(RPES)}{\sigma(RPES)} \times 100\%. \tag{32}$$

Note that the performance index is negative and it takes a lower value for a larger reduction of RPES after compensation.

1) Inverse sensitivity method: An existing technique is called an inverse sensitivity method. In this method, PES is averaged over multiple revolutions of the disk to reduce NRRO effect, and then the averaged PES is filtered by an approximation of the inverse sensitivity function to back calculate the estimated RRO. It is an open loop estimation. Frequency responses of the inverse sensitivity function $S^{-1}(z)$ and its 180-tap FIR approximation $\widehat{S^{-1}}(z)$ are shown in Fig. 6. Since RRO only affects PES at harmonic frequencies $f_k \in \Omega$, $\widehat{S^{-1}}(z)$ is designed to

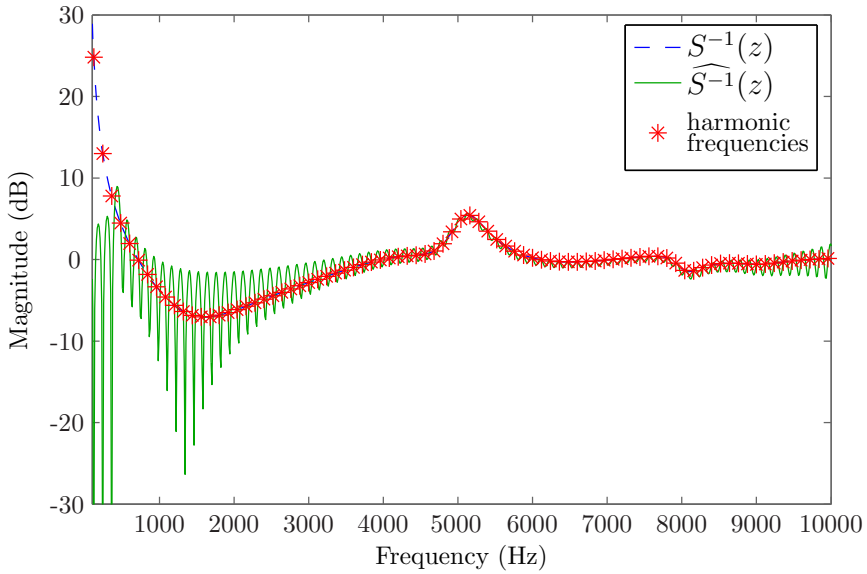

Fig. 6. Frequency response of $S^{-1}(z)$ and $\widehat{S^{-1}}(z)$ in inverse sensitivity method

intersect the frequency response of $S^{-1}(z)$ only at frequencies f_k, except at f_1, f_2 and f_3. The low gain design at these frequencies is to prevent amplification of the low frequency contents in NRRO. The compensation performance of the inverse sensitivity method is plotted in Fig. 7. The solid lines with square markers represent the average performance for 20 tracks, and the dashed lines indicate the performance variance among different tracks. The inverse sensitivity method achieves an average 50% RPES reduction after 8 revolutions as shown in Fig. 7. However, the performance exhibits high variations due to the wide range of the RPES-to-NRPES ratio.

2) Repetitive Control: Since RRO is a periodic disturbance, repetitive control can be applied to estimate RRO at all harmonics of the fundamental frequency. The block diagram of the closed loop system utilizing a repetitive controller is shown in Fig. 8. The repetitive controller contains a stable inverse of the sensitivity function and a periodic signal generator. An adjustable again K_r controls the tradeoff between the convergence rate and estimation accuracy. The inverse sensitivity function in the repetitive control is modeled as a 5th order rational transfer function.

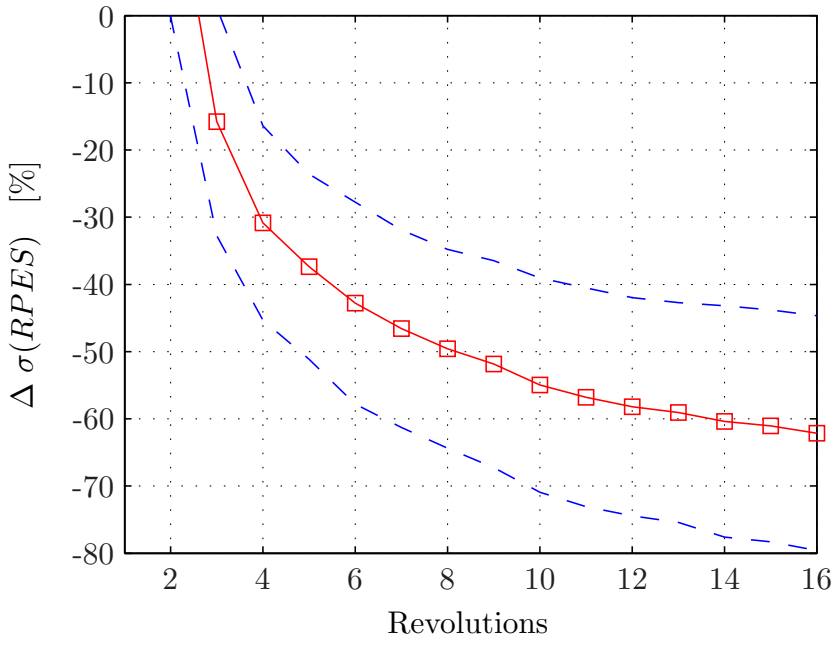

Fig. 7. Compensation performance of inverse sensitivity method

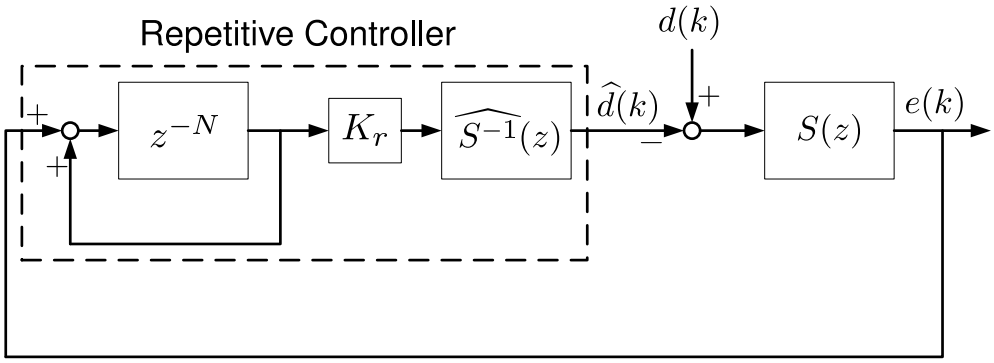

Fig. 8. RRO estimation using a repetitive controller

Its frequency response is shown in Fig. 9. The performance of the system with the repetitive controller is shown in Fig. 10. Since the repetitive controller utilizes the feedback error signal, the closed loop system is more robust to the wide range of the RPES-to-NRPES ratio. The performance variations are smaller than that of the inverse sensitivity method.

3) AFC schemes: The frequency response of the sensitivity function $S(z)$ of the servo system is shown in Fig. 11. Its approximation $\widehat{S}(z)$ employed in the AFC setting is a 10-tap FIR filter.

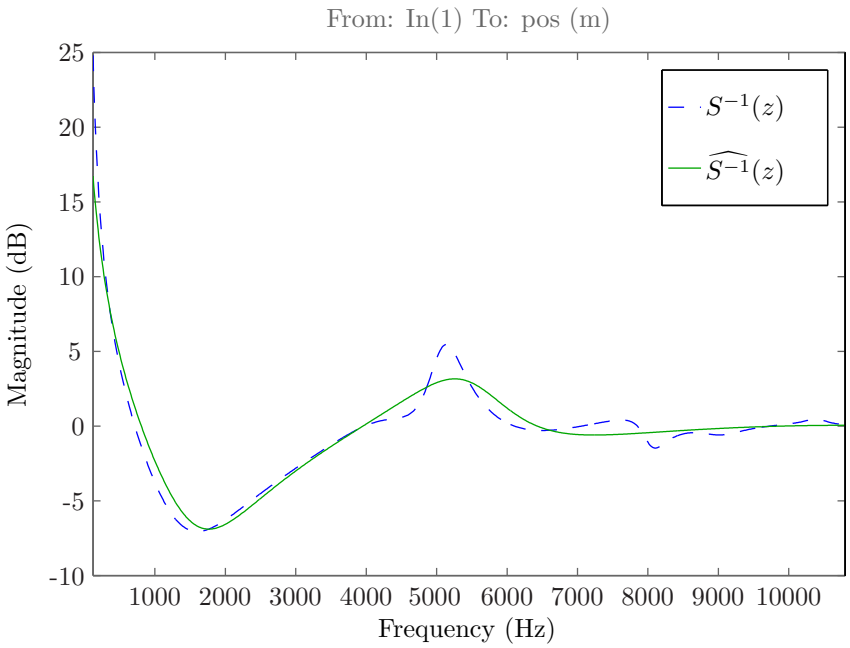

Fig. 9. Frequency response of $S^{-1}(z)$ and $\widehat{S^{-1}}(z)$ in repetitive control

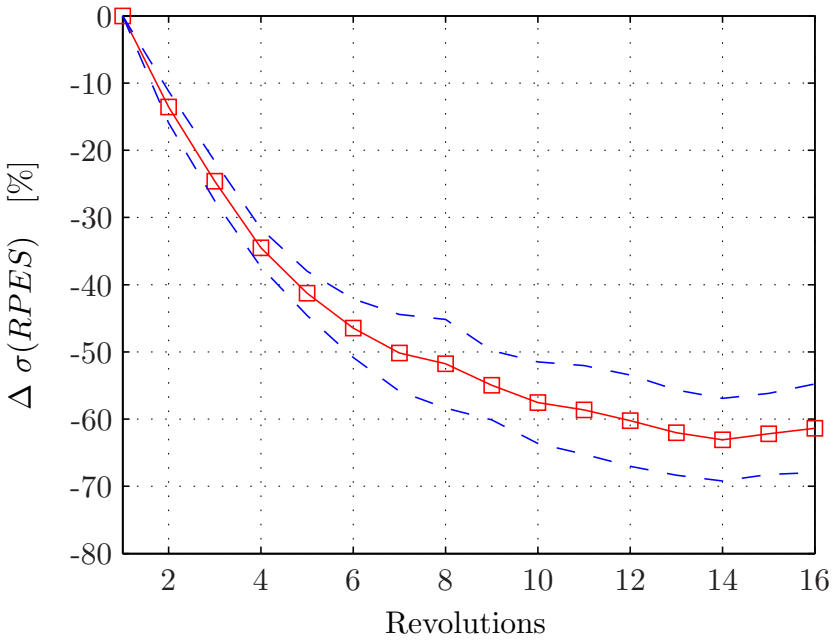

Fig. 10. Compensation performance of repetitive control

From Fig. 12, it is shown that $\widehat{S}(z)$ satisfies the stability condition of the MFX-LMS algorithm in Eq. (28). The Performances of the AFC schemes using FX-LMS and MFX-LMS both with additional Kalman filtering are shown in Figs. 13 and 14. Both methods are robust to different RPES-to-NRPES ratios and result in small performance variations; they are significantly superior to the inverse sensitivity method and better than the repetitive control in terms of performance variations. Table I summarizes the performances among different methods after 8 revolutions. AFC using FX-LMS algorithm reduces RPES by 51%, whereas using MFX-LMS algorithm achieves 59% reduction which is the best of the four. If it is desired to reduce RPES by half, using the proposed MFX-LMS algorithm with Kalman filtering can shorten the estimation period by 2 or 3 revolutions. This means a significant reduction of manufacturing time compared with the inverse sensitivity method, i.e. 25%.

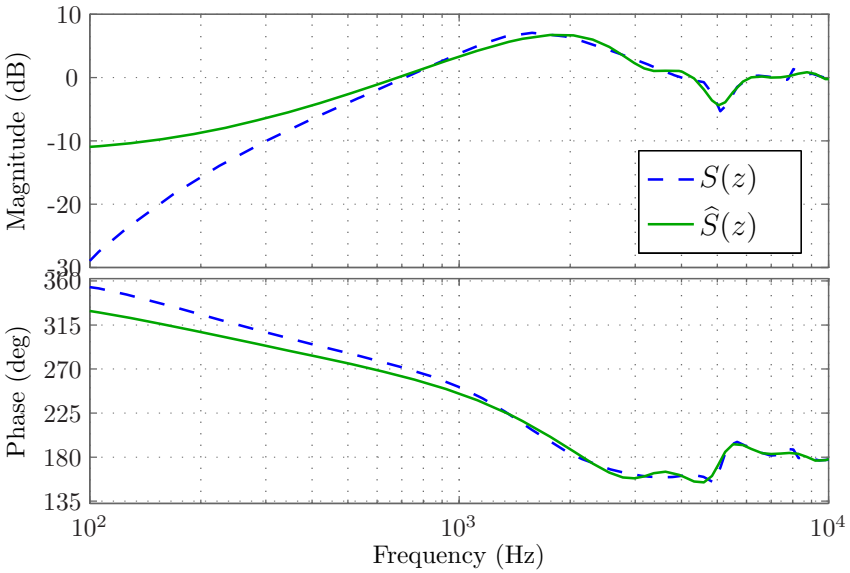

Fig. 11. Frequency response of $S(z)$ and $\widehat{S}(z)$

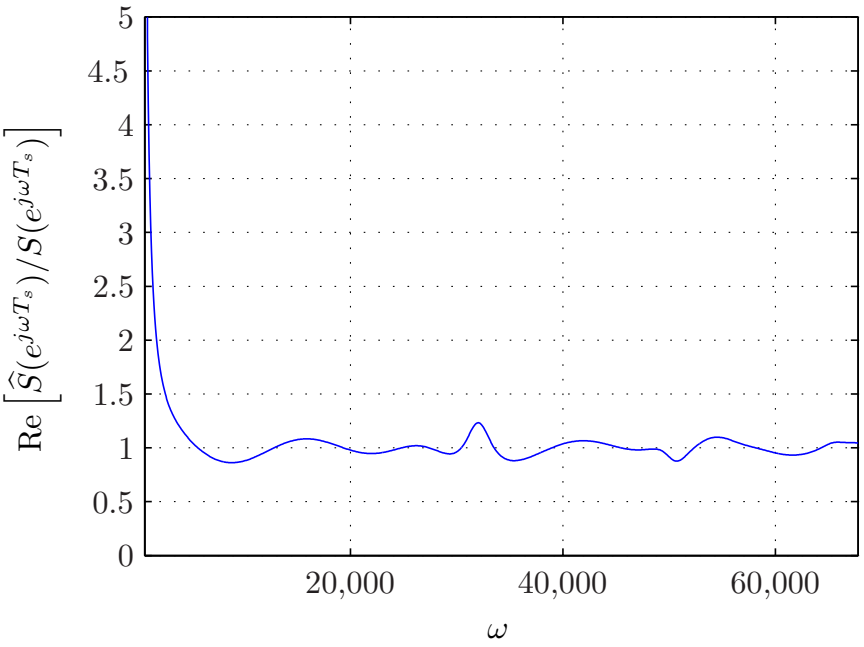

Fig. 12. $\mathfrak{Re}\left[\widehat{S}(e^{j\omega T_s})/S(e^{j\omega T_s})\right]$ v.s. ω

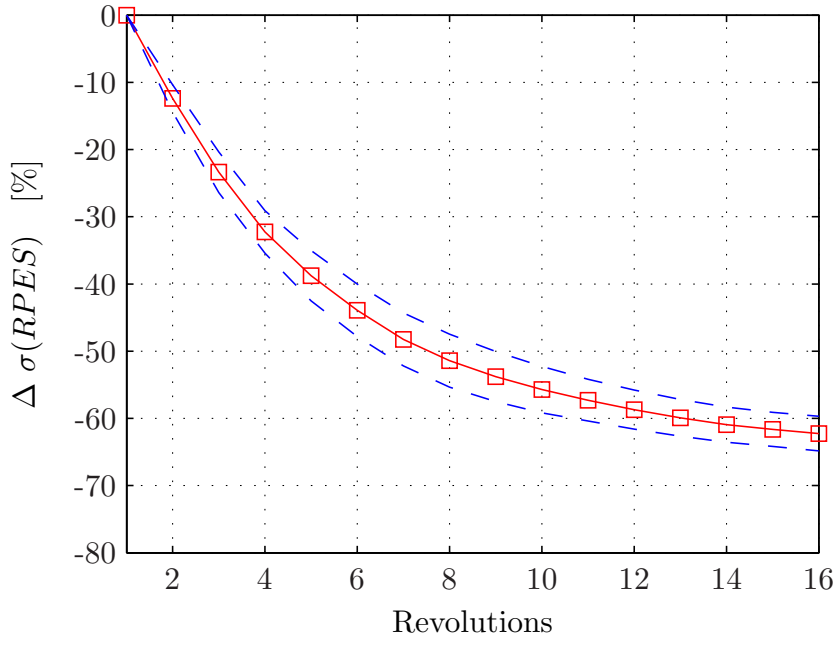

Fig. 13. Compensation performance of FX-LMS with Kalman filter

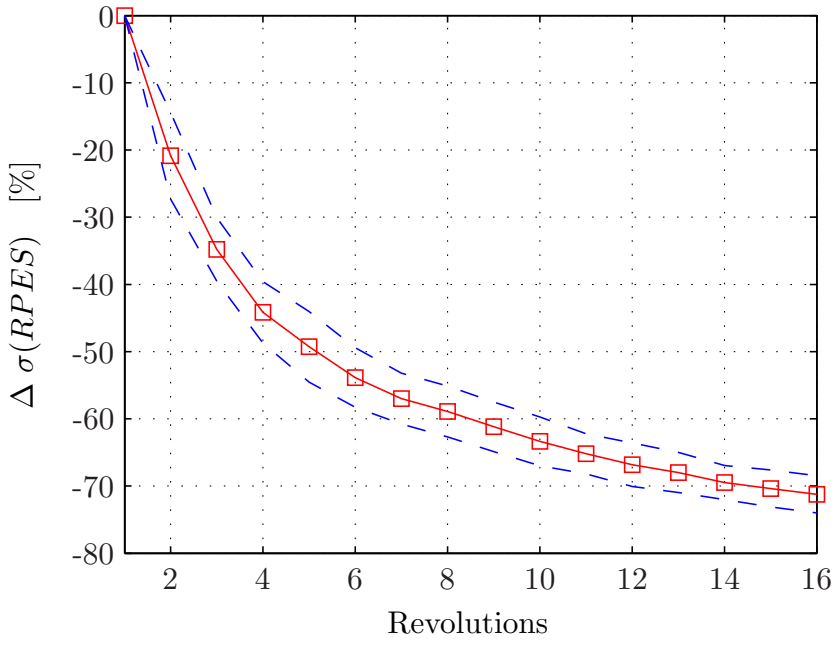

Fig. 14. Compensation performance of MFX-LMS with Kalman filter

TABLE I
PERFORMANCE COMPARISON AFTER 8 REVOLUTIONS

Scheme	Inverse Sensitivity	Repetitive Control	FX-LMS w/ Kalman	MFX-LMS w/ Kalman
$\Delta\ \sigma(RPES)$	-49.58%	-51.77%	-51.41%	-58.92%

IV. FREQUENCY SELECTIVE ESTIMATION

The plant output $y(k)$ in Fig. 2 can be regarded as the True Position Error (TPE) of the R/W head, i.e. the true deviation from the virtual ideal track center. Notice that in practice this signal is unavailable for measurement because of disturbances. The Repeatable TPE (RTPE) caused by RRO disturbance $d(k)$ is given by

$$RTPE(k) = T(z)d(k) = \frac{P(z)C(z)}{1 + P(z)C(z)}d(k) \tag{33}$$

$$RTPE_{cmp}(k) = T(z)\left[d(k) - \widehat{d}(k)\right], \tag{34}$$

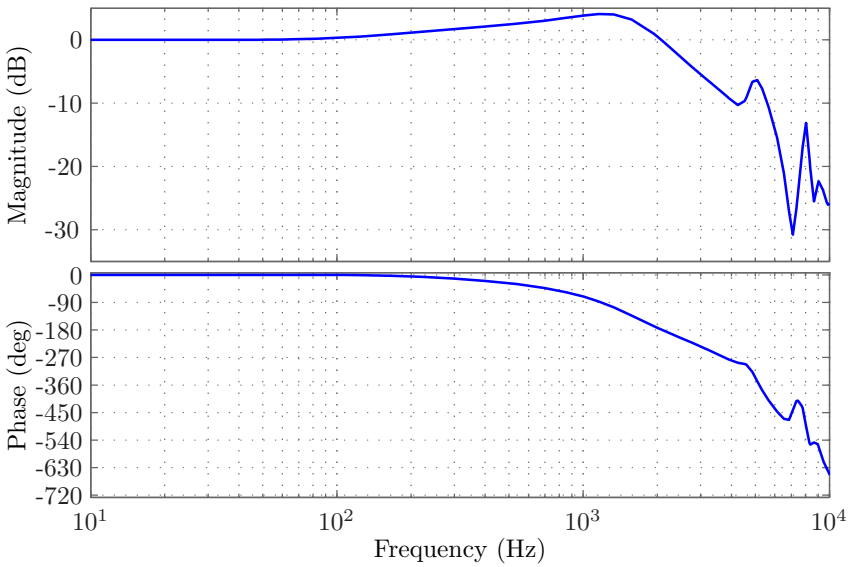

Fig. 15. Frequency response of complimentary sensitivity function $T(z)$

where $T(z)$ is the complimentary sensitivity function of the closed-loop system. Using the same simulation data as in Section III, the frequency response of $T(z)$ of the simulated closed-loop system in Fig. 15 indicates a significant drop of the gain beyond around 5kHz. It means that the R/W head cannot follow the high frequency variations in the servo-written track center due to the limited control bandwidth. Instead, the R/W head moves along a smoothened path. Therefore, the high frequency components of RRO have small impacts on the tracking performance and can be excluded from the estimation. To develop a frequency selective estimation, a straightforward way is to remove the high-frequency components in the error signal $e(k)$ by adding a low-pass filter. This results in an increased computational cost. A more efficient method is to replace the usage of an impulse train in $x(k)$ by a rectangular wave. In this case, $x(k)$ is expressed as

$$x(k) = \begin{cases} 1, & \text{if mod}(k, N) = 0 \text{ or } 1 \\ 0, & \text{otherwise.} \end{cases} \tag{35}$$

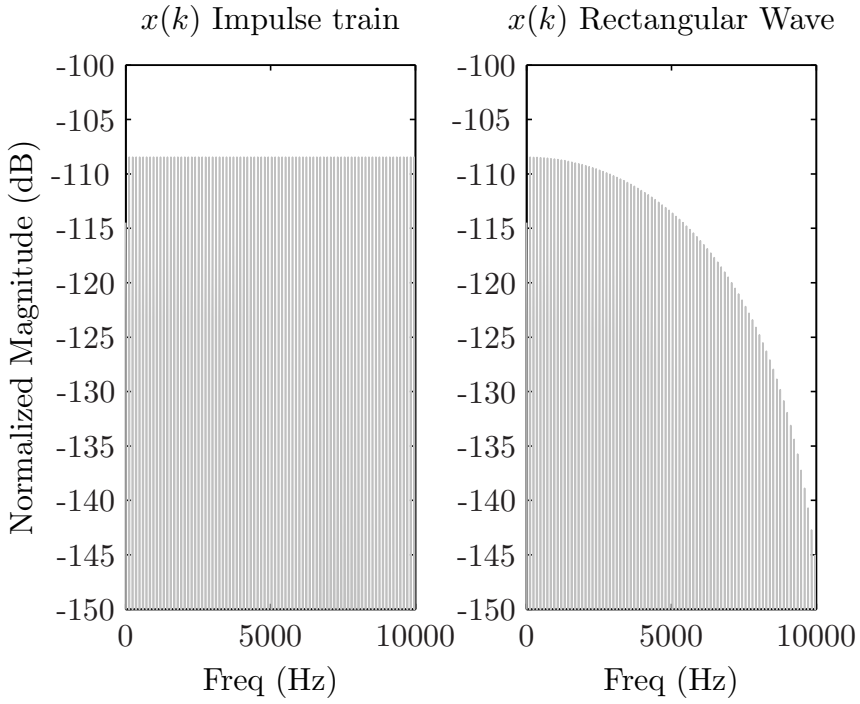

Fig. 16. Spectrum of impulse train and rectangular wave

In Fig. 16, from the spectrum comparison of a impulse train in Eq. (9) and a rectangular wave in Eq. (35), the magnitude of the rectangular wave rolls off at high frequencies. Those frequency components will hardly show up at the adaptive filter output $z(k)$, and thus the frequency selective estimation is accomplished. In general, a rectangular wave designed to contain the necessary harmonics, $f_k, k = 1, \ldots, M$, is given by

$$x(k) = \begin{cases} 1, & \text{if mod}(k, N) = 0, \ldots, N_1 \\ 0, & \text{otherwise.} \end{cases} \tag{36}$$

where

$$\frac{N_1}{N} \leq \frac{1}{2M} \tag{37}$$

A new performance index is needed for the frequency selective scheme. It is defined as

$$\Delta\ \sigma(RTPE) = \frac{\sigma(RTPE_{cmp}) - \sigma(RTPE)}{\sigma(RTPE)} \times 100\%, \tag{38}$$

In simulation studies, RTPE reduction can be observed. Comparing the performances of the proposed AFC scheme using an impulse train and a rectangular wave in Figs. 17 and 18, the latter achieves a larger RTPE reduction and smaller performance variations. Spectrum of the estimate $\widehat{d}(k)$ compared with that of $d(k)$ is shown in Fig. 19. It is observed that the frequency components beyond 5kHz are excluded in the estimation process and do not show up in $\widehat{d}(k)$. Because the number of frequency components required to be estimated is lesser, the proposed AFC scheme using a rectangular wave can achieve faster and more accurate estimation and thus a greater reduction of RTPE. In other words, the R/W head can follow the ideal circular track center more closely.

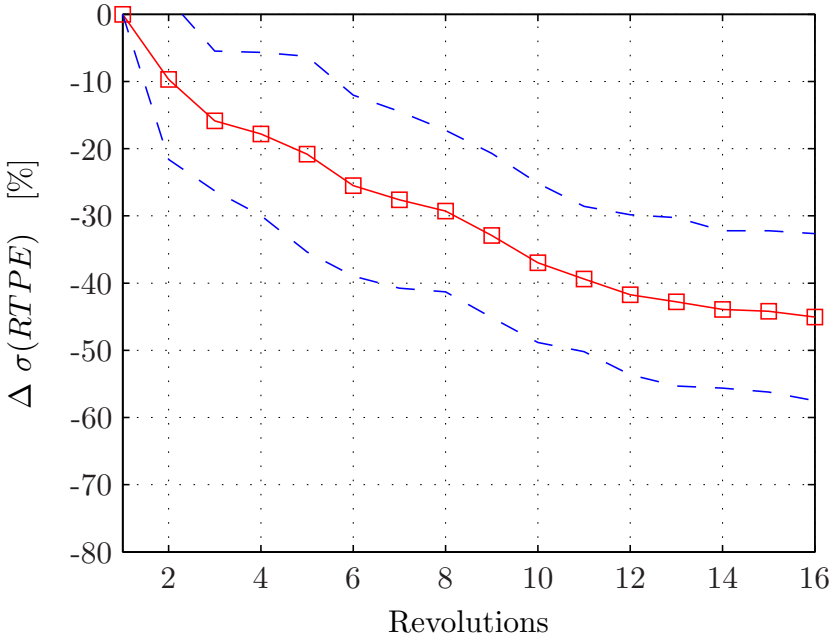

Fig. 17. Compensation performance using impulse train

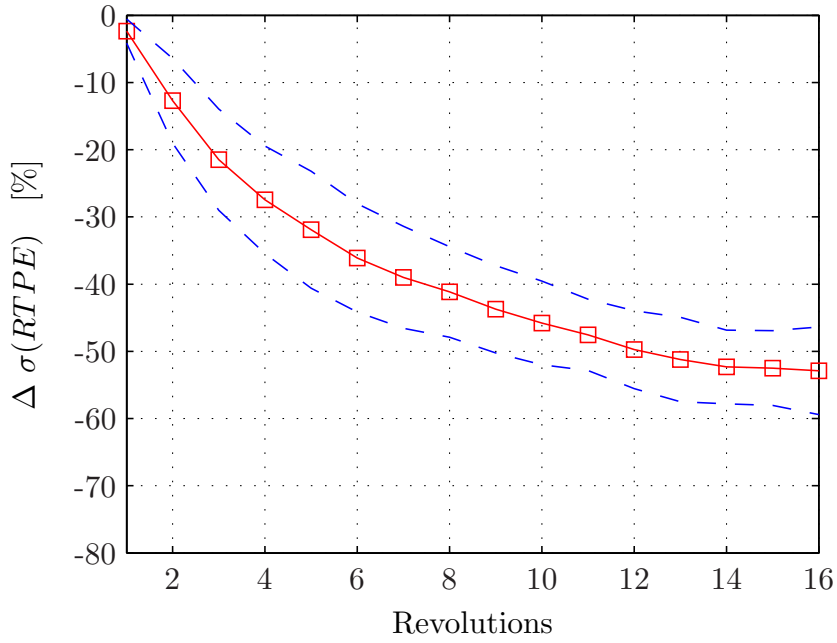

Fig. 18. Compensation performance using rectangular wave

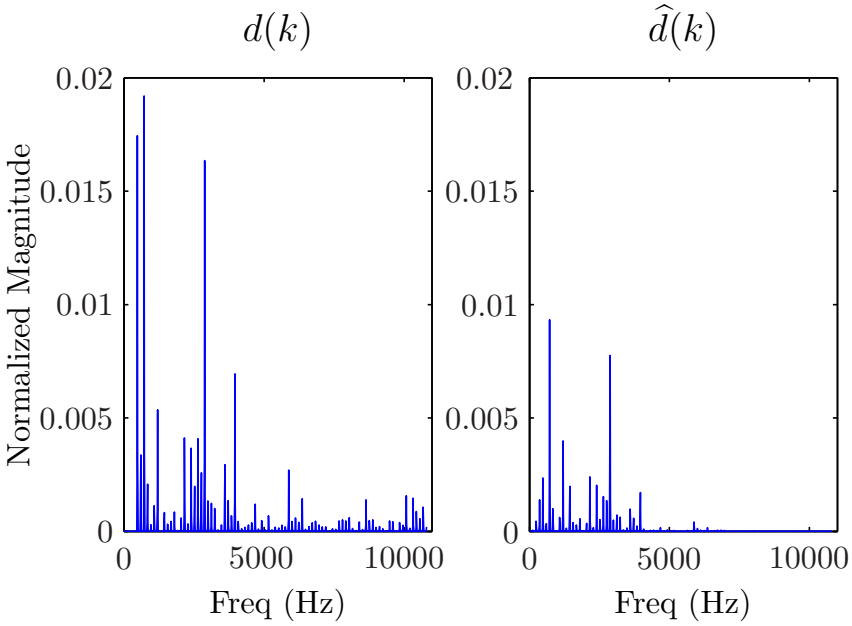

Fig. 19. Spectrum of $d(k)$ and $\widehat{d}(k)$

V. Conclusions

This report discussed the RRO estimation methods used for RRO cancellation. The adaptive feedforward compensation scheme with MFX-LMS algorithm was applied to estimate RRO. Kalman filtering was introduced to enhance the performance of AFC. The proposed method was compared with two common methods: the inverse sensitivity method and the repetitive control method. In addition, a frequency selective estimation scheme was introduced to exclude the high frequency components of the RRO disturbance. It was achieved by choosing a different input signal in AFC. The simulation results showed the effectiveness of the proposed methods and the improvement of the tracking performance.

ACKNOWLEDGMENTS

This research was supported by the Computer Mechanics Laboratory (CML) in the Department of Mechanical Engineering, University of California at Berkeley. The authors thank Dr. Li Yi for useful discussions.

REFERENCES

[1] K. K. Chew and M. Tomizuka, “Digital control of repetitive errors in disk drive systems,” *IEEE Control Systems Magazine*, vol. 10, no. 1, pp. 16–20, 1990.

[2] A. Sacks, M. Bodson, and P. Kholsa, “Experimental results of adaptive periodic disturbance cancellation in a high performance magnetic disk drive,” in *American Control Conference*, vol. 2, 1993, pp. 686–690.

[3] A. Sacks, M. Bodson, and W. Messner, “Adaptive methods for repeatable runout compensation,” *IEEE Transactions on Magnetics*, vol. 31, no. 2, pp. 1031–1036, 1995.

[4] M. Kawafuku, M. Iwasaki, H. Hirai, M. Kobayashi, and A. Okuyama, “Rejection of repeatable runout for HDDs using adaptive filter,” in *Proc. of International Workshop on Advanced Motion Control*, 2004, pp. 305–310.

[5] Y. Chen, L. Tan, K. Ooi, Q. Bi, and K. Cheong, “Repeatable runout disturbance compensation using a learning algorithm with scheduled parameters,” U.S. Patent 6 437 936.

[6] Q. W. Jia, Z. F. Wang, and F. C. Wang, “Repeatable runout disturbance compensation with a new data collection method for hard disk drive,” *IEEE Transactions On Magnetics*, vol. 41, no. 2, pp. 791–796, 2005.

[7] S.-C. Wu and M. Tomizuka, “Repeatable runout compensation for hard disk drives using adaptive feedforward cancellation,” in *American Control Conference*, 2006, pp. 382–387.

[8] ——, “Repeatable runout compensation for hard disk drives using adaptive feedforward cancellation,” Univ. of California at Berkeley,” Computer Mechanics Laboratory (CML) Technical Report, December 2005.

[9] S. J. Elliot and P. A. Nelson, “Active noise control,” *IEEE Signal Processing Mag.*, vol. 10, pp. 12–35, 1993.

[10] M. Rupp and A. H. Sayed, “Modified FXLMS algorithms with improved convergence performance,” in *Proc. 29th Asilomar Conf. Signals, Systems, Computers*, vol. 2, 1995, pp. 1255–1259.

[11] P. A. C. Lopes and M. S. Piedade, “The behavior of the Modified FX-LMS algorithm with secondary path modeling errors,” *IEEE signal processing letters*, vol. 11, no. 2, pp. 148–151, 2004.